Binding of Influenza Virus Hemagglutinin to Analogs of Its Cell-Surface Receptor, Sialic Acid: Analysis by Proton Nuclear Magnetic Resonance Spectroscopy and X-ray Crystallography†

Nicholas K. Sauter,‡,§,‖ John E. Hanson,‡,‖,⊥ Gary D. Glick,#,△ Jerry H. Brown,‡ Robert L. Crowther,‡ Seong-Joon Park,‡ John J. Skehel,○ and Don C. Wiley*,‡,∞

Department of Biochemistry and Molecular Biology, Howard Hughes Medical Institute, and Department of Chemistry, Harvard University, Cambridge, Massachusetts 02138, and National Institute for Medical Research, London NW7 1AA, United Kingdom

Received April 8, 1992; Revised Manuscript Received July 22, 1992

ABSTRACT: The interaction between influenza virus hemagglutinin and its cell-surface receptor, 5-*N*-acetylneuraminic acid (sialic acid), was probed by the synthesis of 12 sialic acid analogs, including derivatives at the 2-carboxylate, 5-acetamido, 4-, 7-, and 9-hydroxyl, and glycosidic positions. The equilibrium dissociation constants of these analogs were determined by nuclear magnetic resonance spectroscopy. Ligand modifications that reduced or abolished binding included the replacement of the 2-carboxylate with a carboxamide, the substitution of azido or *N*-benzyloxycarbonyl groups for the 5-acetamido group, and the replacement of the 9-hydroxyl with amino or *O*-acetyl moieties. Modifications having little effect on binding included the introduction of longer chains at the 4-hydroxyl position, the replacement of the acetamido methyl group with an ethyl group, and the removal of the 7-hydroxyl group. X-ray diffraction studies yielded 3 Å resolution crystal structures of hemagglutinin in complex with four of the synthetic analogs [α-2-*O*-methyl-, 4-*O*-acetyl-α-2-*O*-methyl-, 9-amino-9-deoxy-α-2-*O*-methyl-, and α-2-*O*-(4′-benzylamidocarboxybutyl)-*N*-acetylneuraminic acid] and with the naturally occurring cell-surface saccharide (α2–3)sialyllactose. The X-ray studies unambiguously establish the position and orientation of bound sialic acid, indicate the position of the lactose group of (α2–3)sialyllactose, and suggest the location of an α-glycosidic chain (4′-benzylamidocarboxybutyl) that increases the binding affinity of sialic acid by a factor of about 3. Although the protein complexed with α-2-*O*-methylsialic acid contains the mutation Gly-135 → Arg near the ligand binding site, the mutation apparently does not affect the ligand's position. The X-ray studies allow us to interpret the binding affinities in terms of the crystallographic structure. The results suggest further experiments which could lead to the design of tight binding inhibitors of possible therapeutic value.

During influenza infection, the virus attaches to cell-surface receptors containing sialic acids (reviewed by Paulson (1985)). α-Glycosides of sialic acid are recognized by hemagglutinin, the viral membrane glycoprotein that mediates both the initial attachment of virus to target cells and the subsequent fusion of the viral and cell membranes (reviewed by Wiley and Skehel (1987)).

The nature of the hemagglutinin–sialic acid interaction has been illuminated by a variety of binding experiments. Viral specificity for different cell-surface receptors was investigated by hemagglutination studies, in which erythrocytes were derivatized with sialic acids linked to the cell surface through either (α2–6)- or (α2–3)glycosidic bonds (Carroll et al., 1981). Hemagglutination has also been observed using erythrocytes where the parent sialic acid, 5-*N*-acetylneuraminic acid (Neu5Ac[1]), was replaced with other naturally occurring analogs (Higa et al., 1985) or where the sialic acids were modified by periodate oxidation (Suttajit & Winzler, 1971; Underwood et al., 1987). The affinities of soluble sialic acid analogs for hemagglutinin were determined by their ability to inhibit viral attachment to cells (Pritchett, 1987; Pritchett et al., 1987; Kelm et al., 1992) or their ability to inhibit hemagglutination (Toogood et al., 1991). Finally, ^{1}H NMR was used to measure binding affinities of hemagglutinin and sialic acid analogs in a cell-free environment (Sauter et al., 1989).

An atomic model of the hemagglutinin–sialic acid interaction emerged from X-ray crystallographic studies that yielded the three-dimensional structure of hemagglutinin from the 1968 Hong Kong epidemic (Wilson et al., 1981) and structures of three isomorphous proteins containing single amino acid mutations (Knossow et al., 1984, 1986; Weis et al., 1988, 1990a, 1990b). Sialic acid analogs bind to two distinct sites on the protein: a first site located in a surface pocket of hemagglutinin's HA1 polypeptide chain (Weis et

† Postdoctoral fellowship support was received from the National Institutes of Health (G.D.G.), and predoctoral fellowship support was received from the Howard Hughes Medical Institutes (S.-J.P.). Organic synthesis were supported by National Institutes of Health Grant GM-39589 to Jeremy R. Knowles and D.C.W., and X-ray studies were supported by National Institutes of Health Grant AI-13654 to D.C.W.

* Author to whom correspondence should be addressed.

‡ Department of Biochemistry and Molecular Biology, Harvard University.

§ Present address: Department of Biochemistry and Biophysics, University of California, San Francisco, CA 94143-0448.

‖ Both authors contributed equally to this paper and should be considered as first authors.

⊥ Present address: Department of Chemistry, University of Puget Sound, Tacoma, WA 98416.

Department of Chemistry, Harvard University.

△ Present address: Department of Chemistry, University of Michigan, Ann Arbor, MI 48109.

○ National Institute for Medical Research.

∞ Howard Hughes Medical Institute, Harvard University.

[1] Abbreviations: Neu5Ac, 5-*N*-acetylneuraminic acid; (α2–3)sialyllactose, Neu5Ac(α2–3)Gal(β1–4)Glc; (α2–6)sialyllactose, Neu5Ac(α2–6)Gal(β1–4)Glc; G135R, X-31 hemagglutinin containing the mutation Gly-135 → Arg; BHA, bromelain-released hemagglutinin; Neu5Acα2Me, α-2-*O*-methyl-5-*N*-acetylneuraminic acid; Neu5Acα2Bac, α-2-*O*-(4′-benzylamidocarboxybutyl)-5-*N*-acetylneuraminic acid.

0006-2960/92/0431-9609$03.00/0

al., 1988) and a second site located at the interface between the HA1 and HA2 polypeptide chains (Sauter et al., 1992). The following results suggest that the first site is the major determinant of cell recognition. (1) The first site is composed of residues conserved in all known sequences of influenza A hemagglutinins (Wilson et al., 1981). (2) An amino acid mutation in the first site changes the binding specificity in viral agglutination experiments; viruses with hemagglutinin HA1 containing Leu-226 preferentially agglutinate erythrocytes derivatized with Neu5Ac(α2–6)Gal(β1–4)GlcNAc, while viruses with hemagglutinin HA1 containing Gln-226 preferentially agglutinate erythrocytes derivatized with Neu5Ac(α2–3)Gal(β1–3)GalNAc (Rogers et al., 1983). (3) Crystallographic experiments with cell-surface oligosaccharides show that Neu5Ac(α2–6)Gal(β1–4)Glc [(α2–6)sialyllactose] binds only to the first site, while Neu5Ac(α2–3)Gal(β1–4)Glc [(α2–3)sialyllactose] binds to the first site with at least 4 times higher affinity than to the second site (Sauter et al., 1992).

One approach in the design of high-affinity inhibitors is to use Neu5Ac as a scaffolding, modifying its functional groups in order to increase its affinity. We have investigated the sialic acid analogs listed in Figure 1 in order to evaluate how important individual functional groups of Neu5Ac are to the overall binding reaction and to help interpret this information in terms of the three-dimensional structural features of the first binding site.[2] These experiments deal with an aspect of inhibitor design distinct from that addressed by studies involving multisialyllated molecules, including the sialyl glycoprotein α_2-macroglobulin (Pritchett & Paulson, 1989), synthetic polymers carrying pendant α-sialosides (Matrosovich et al., 1990; Spaltenstein & Whitesides, 1991; Gamian et al., 1991), and bivalent sialosides (Glick & Knowles, 1991; Sabesan et al., 1991b; Glick et al., 1991). Many of these multivalent compounds exhibit high inhibitor potency, probably reflecting the statistical cooperativity of multiple sialic acid binding interactions between the molecule and the virus. This paper, in contrast, seeks to study what is necessary to increase the intrinsic affinity of a single sialic acid molecule for the first binding site of hemagglutinin.

EXPERIMENTAL PROCEDURES

Protein. Studies were performed using two influenza A hemagglutinin variants differing in amino acid sequence only at position 135 of HA1. Hemagglutinin containing Gly-135 (Verhoeyen et al., 1980) was obtained from the recombinant viral strain X-31 that carries hemagglutinin from the A/Aichi/2/1968 (H3N2) isolate. Protein containing Arg-135 (G135R) was derived from an antigenic variant of the X-31 virus selected with monoclonal antibodies (Daniels et al., 1983; Underwood et al., 1987). The soluble extracellular domain of hemagglutinin was proteolytically released from the virus (Brand & Skehel, 1972), and the resulting bromelain-released hemagglutinin (BHA) was cleared of residual neuraminidase activity by immunoaffinity chromatography (Sauter et al., 1989; Sauter, 1991). For NMR binding experiments, protein was dialyzed into a deuterated buffer as described (Sauter et al., 1989). For crystallographic studies, crystals of space group $P4_1$ were grown by microdialysis or vapor diffusion against 1.3–1.55 M sodium citrate and 0.1% sodium azide, pH 7.5,

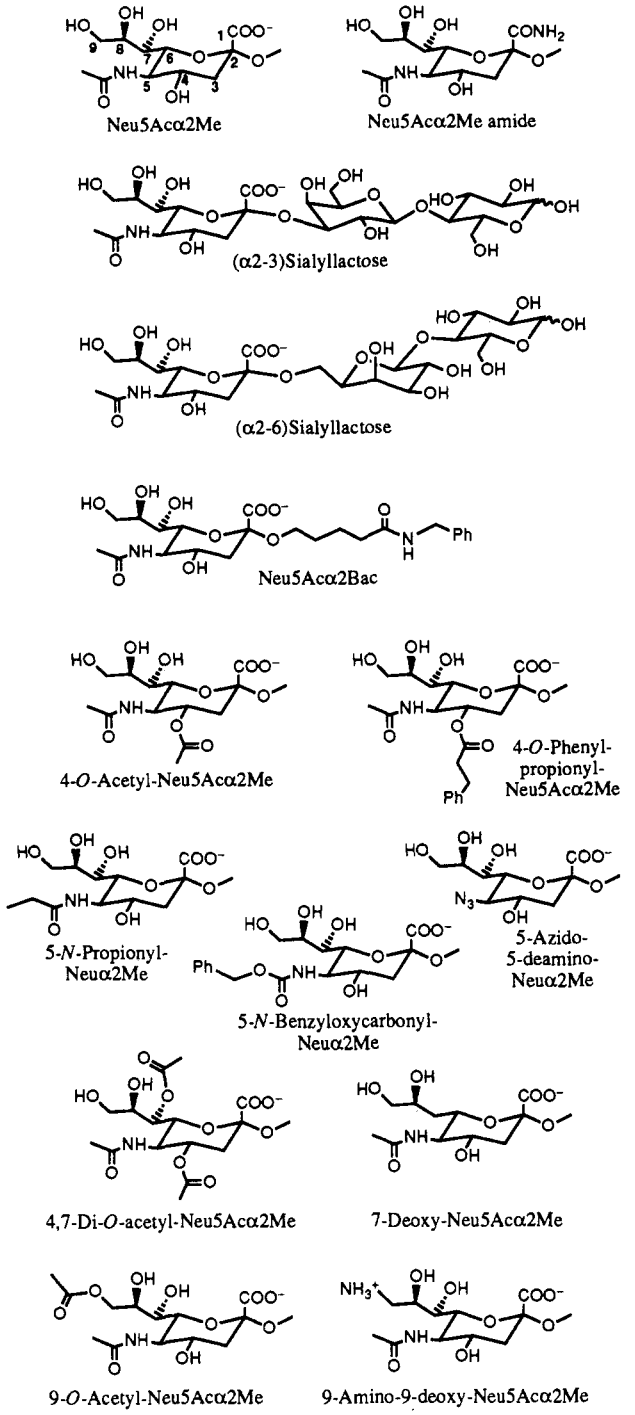

FIGURE 1: Structural formulas for the Neu5Ac analogs studied. The symbol Ph represents the phenyl group, C_6H_5.

and were isomorphous to crystals examined previously (Wiley & Skehel, 1977; Wilson et al., 1981; Knossow et al., 1984; Weis et al., 1988).

Ligands. Structural formulas for the ligands studied are given in Figure 1. Salts of (α2–3)- and (α2–6)sialyllactose were purchased from Biocarb Chemicals (Lund, Sweden) and used for the NMR studies. For the crystallographic experiment, (α2–3)sialyllactose was isolated by HPLC (Bergh, 1981; Sauter, 1991) from a mixture of (α2–3) and (α2–6) isomers from bovine colostrum (Sigma). Chemical syntheses for α-2-*O*-methyl-5-*N*-acetylneuraminic acid (Neu5Acα2Me), 4-*O*-acetyl-Neu5Acα2Me, 4,7-di-*O*-acetyl-Neu5Acα2Me (Sauter et al., 1989), and α-2-*O*-4′-(benzylamidocarboxybutyl)-5-*N*-acetylneuraminic acid (Neu5Acα2Bac; Toogood et al., 1991) were performed as described. 5-Azido-5-deamino-

[2] Atomic coordinates and structure factor amplitudes have been deposited in the Protein Data Bank, Chemistry Department, Brookhaven National Laboratory, Upton, NY 11973 (reference numbers 1HGD-1HGJ, R1HGDSF-R1HGJSF).

Table I: Dissociation Constants[a] in D_2O (297 ± 1 K)

compound	X-31 BHA			G135R BHA		
	K_D (mM)[a]	[protein] (μM)[f]	$\Delta\delta_{Bapp}$ (ppm)[b]	K_D (mM)[a]	[protein] (μM)[f]	$\Delta\delta_{Bapp}$ (ppm)[b]
Neu5Acα2Me	2.8[c]	33	2.1	5.4	31	2.3
(α2–6)sialyllactose	2.1[c]	25, 49	1.5, 1.9	3.7	33	1.9
(α2–3)sialyllactose	3.2[c]	37	1.9	4.2	33	2.0
Neu5Acβ2Me	ND[d](>200)[c]	150				
Neu5Acα2Me amide	ND[d] (>100)	37				
Neu5Acα2Bac	1.4[e]	15	1.1			
4-*O*-acetyl-Neu5Acα2Me	2.1[c]	42	1.5			
4-*O*-phenylpropionyl-Neu5Acα2Me	2.8	29	1.7			
5-*N*-propionyl-Neuα2Me	3.8	34	CH_2 = 0.91 CH_3 = 1.5			
5-*N*-(benzyloxycarbonyl)Neuα2Me	ND[d](>20)	33				
5-azido-5-deamino-Neuα2Me	ND[d](>40)	57				
4,7-di-*O*-acetyl-Neu5Acα2Me	ND[d](>100)[c]	63				
7-deoxy-Neu5Acα2Me	6.5	34	2.6			
9-*O*-acetyl-Neu5Acα2Me	ND[d](>100)	58				
9-amino-9-deoxy-Neu5Acα2Me	22	86	1.0			

[a] Unless otherwise noted, the dissociation constants shown are weighted averages of the results from analysis of various resonances. The estimated uncertainty in the values of the dissociation constants is ±20%. [b] The apparent chemical shift change for the *N*-acetyl methyl resonance upon binding to hemagglutinin, as in eq 1 of Sauter et al. (1989). For the *N*-propionyl derivative, the apparent shift changes for the *N*-propionyl methylene and methyl resonances are shown. [c] From Sauter et al. (1989). [d] No detectable binding. The estimated limit of detection is given in parentheses. [e] This is the value calculated from the *N*-acetyl shift data only; the dissociation constants calculated from line broadening of four other resonances varied from 0.6 to 0.9 mM. [f] Number of protein binding sites calculated using an extinction coefficient of 1.5 cm^{-1} $(mg/mL)^{-1}$ and a monomer molecular weight of 69 500 (Sauter et al., 1989).

Neuα2Me was a gift from Dr. Andreas Schrell and Dr. George Whitesides. The amide derivative of Neu5Acα2Me was prepared from the corresponding methyl ester (van der Vleugal et al., 1982) by stirring overnight in a solution of ammonia in methanol.

The synthesis of the 4-*O*-phenylpropionyl derivative of Neu5Acα2Me was similar to that described for the 4-*O*-acetyl derivative (Sauter et al., 1989). The methyl ester of Neu5Acα2Me was converted to the benzyl ester by treatment with catalytic potassium *tert*-butoxide in benzyl alcohol. Treatment of the benzyl ester with 2,2-dimethoxypropane and acetone in the presence of Dowex 50W (H^+) afforded the 8,9-*O*-isopropylidene derivative, which was subsequently acylated at the 4-position by addition of 3-phenylpropionyl chloride to a solution of this derivative in pyridine in the presence of 4-(dimethylamino)pyridine. Removal of the 8,9-acetonide by heating with 80% acetic acid, followed by hydrogenolysis with 10% Pd/C catalyst to remove the benzyl ester, produced 4-*O*-phenylpropionyl-Neu5Acα2Me.

5-*N*-(Benzyloxycarbonyl)-Neuα2Me was prepared from the corresponding methyl ester (a gift from Mr. Greg Priebe and Dr. George Whitesides) by hydrolysis with sodium hydroxide. 5-*N*-propionyl-Neuα2Me was also prepared from the methyl ester of 5-*N*-(benzyloxycarbonyl)-Neuα2Me by (1) treatment with hydrogen and 10% Pd/C to remove the benzyloxycarbonyl group, (2) acylation of the 5-amino group with propionic anhydride, and (3) hydrolysis of the methyl ester with sodium hydroxide.

The synthesis of 7-deoxy-Neu5Acα2Me was analogous to that described by Zbiral et al. (1988) for preparation of the 7-deoxy derivative of Neu5Ac. The 4-hydroxyl of 8,9-*O*-isopropylidene-Neu5Acα2Me benzyl ester was protected as its 4-*tert*-butyldimethylsilyl ether. The 7-hydroxyl was then converted to its xanthate ester by deprotonation with butyllithium, treatment with carbon disulfide, and alkylation with methyl iodide. Deoxygenation of the 7-position was accomplished by heating with tributyltin hydride in xylenes. Removal of the 8,9-acetonide and the 4-*O*-*tert*-butyldimethylsilyl ether by heating in 80% acetic acid, followed by hydrogenolysis to remove the benzyl ester, afforded 7-deoxy-Neu5Acα2Me.

The 9-*O*-acetyl derivative of Neu5Acα2Me was readily prepared from Neu5Acα2Me benzyl ester by selective acylation with acetyl chloride in pyridine followed by hydrogenolysis to remove the benzyl ester.

Synthesis of 9-amino-9-deoxy-Neu5Acα2Me was also straightforward. Reaction of Neu5Acα2Me benzyl ester with *p*-toluenesulfonyl chloride in pyridine produced the 9-*O*-tosyl derivative, which was converted to the 9-azido derivative by heating with sodium azide in DMF. Treatment with hydrogen and 10% Pd/C simultaneously removed the benzyl ester and reduced the azido group to the amine, affording the desired 9-amino-9-deoxy-Neu5Acα2Me.

Experimental details, including ^1H and ^{13}C NMR data for all intermediates, may be found in the supplementary material.

NMR Binding Experiments. The NMR binding experiments were conducted and analyzed as described previously (Sauter et al., 1989). Protein concentrations used in the binding assays are shown in Table I. Ligand concentrations ranged from 0.2 to 30 mM, with any particular assay typically spanning a 50-fold concentration range.

Crystallographic Data Collection. Protein/ligand complexes were prepared by soaking crystals in ligand solutions (in 1.36–1.42 M sodium citrate) for 1–5 days prior to X-ray studies (Sauter, 1991). Crystals were chilled to 4 °C, and X-ray diffraction data (Table II) were either recorded on film using 1° oscillation photographs and processed as described (Wilson et al., 1981; Knossow et al., 1984; Weis, 1987; Weis et al., 1988; Brown, 1991) or recorded by a multiwire area detector using 0.04–0.1° oscillation frames and processed with the BUDDHA software package (Durbin et al., 1986; Blum et al., 1987).

Crystallographic Structure Modeling. Details of the model building and refinement methods have been described elsewhere (Sauter, 1991). Briefly, models were refined using the program X-PLOR (Brünger, 1990) as published (Weis et al., 1990a), and the final statistics are listed in Table III. Noncrystallographic 3-fold symmetry restraints were applied to non-hydrogen atoms, with the exception of atoms near lattice contacts (where $2F_{obsd} - F_{calcd}$ maps suggested differences in the three monomers) and residues in the disordered N-terminal of HA1. No monomer-to-monomer differences were observed

Table II: Data Collection Statistics

	ligand concn (mM)	crystals	X-ray source, detector[a]	measurements[b]	unique reflections[c]	R_{merge}[d] (%)
A. X-31 BHA						
4-*O*-acetyl-Neu5Acα2Me	25	16	GX-13, a.d.	166 296	71 877	12.5
(α2–3)sialyllactose	30	6	GX-6,film/GX-13, a.d.	148 649	70 918	13.7
Neu5Acα2Bac	25	15	GX-13, a.d.	157 204	85 146	8.7
9-amino-9-deoxy-Neu5Acα2Me	200	8	GX-13, a.d.	186 422	84 431	9.3
B. G135R BHA						
native		12	DESY/GX-6,film/GX-13, a.d.	245 522	85 025	12.8
Neu5Acα2Me	100	7	GX-13, a.d.	170 719	82 887	10.4

[a] GX-13 and GX-6, Enraf-Nonius rotating anodes; a.d., multiwire area detector; DESY, Deutches Elektronen Synchrotron with film detection. [b] For film data, partial measurements were included if they were >70% recorded. [c] Reflections were rejected if $I < 0$ or tested for rejection if $|I^{hkl}_{obsd} - \langle I^{hkl}\rangle|/\sigma(I^{hkl}_{obsd}) > 3$, where I is intensity and σ is the standard deviation. [d] $R_{merge} = (\sum_{obsd}\sum_{hkl}|I^{hkl}_{obsd} - \langle I^{hkl}\rangle|)/(\sum_{obsd}\sum_{hkl}I^{hkl}_{obsd})$. Data were scaled and merged using the CCP4 program suite.

Table III: Refinement Statistics

	reflections[a]	maximum resolution (Å)	fraction complete[b] (%)	unit cell dimensions *a,c* (Å)	non-hydrogen atoms	R^c (%)	optimal F_o/F_c ratio[d]	bond length rms deviation from ideality (Å)[e]
A. X-31 BHA								
native	65 804	3.00	82.0	163.2,177.4	12 144	23.0	1.095	0.015
4-*O*-acetyl-Neu5Acα2Me	63 509	2.71	74.6	162.7,178.2	12 291	22.3	1.125	0.015
(α2–3)sialyllactose	64 393	2.91	76.8	162.7,177.5	12 474	22.9	1.125	0.014
Neu5Acα2Bac	73 501	2.70	78.6	162.8,178.1	12 348	22.6	1.140	0.015
9-amino-9-deoxy-Neu5Acaα2Me	73 370	2.70	82.5	162.8,177.5	12 282	22.0	1.141	0.014
B. G135R BHA								
native	74 380	2.69	82.3	163.3,176.7	12 237	22.4	1.137	0.014
Neu5Acα2Me	70 578	2.60	80.9	163.1,176.9	12 303	22.5	1.127	0.015

[a] Number of reflections used for X-PLOR refinement; minimum resolution was 7.0 Å. [b] Percent of possible reflections in the resolution range from 7.0 to 3.0 Å. [c] $R = \sum_{hkl}||F^{hkl}_{obsd}| - |F^{hkl}_{calcd}||/\sum_{hkl}|F^{hkl}_{obsd}|$. [d] From X-PLOR refinement. [e] rms deviations from ideality for other geometric quantities were as follows: bond angles, 2.9°; dihedral angles, 25.1–25.4°; peptide bond dihedral angles, 4.6–4.8°; improper dihedral angles, 1.4°. For those parts of the model subject to noncrystallographic symmetry restraints, rms deviation from superposition ranged from 0.026 to 0.030 Å. During refinement, an overall weighting factor W_A = 800 000 (825 000 for native X-31) was applied to the X-ray energy term.

in the vicinity of either sialoside binding site. Since the structure of uncomplexed X-31 BHA (Wilson et al., 1981) has not been previously refined, it was necessary to refine it for this project, taking starting coordinates from the X-PLOR-refined G146D mutant (Weis et al., 1990a). The initial model was subjected to one round of simulated annealing refinement, in which the molecular dynamics temperature was slowly cooled from 2000 to 300 K. Although this protocol produced some improvements in the model, it also caused less ordered parts of the structure to diverge from the electron density. Therefore, after one round of manual rebuilding, all subsequent refinement was performed with alternating cycles of conventional positional minimization and *B* factor refinement. For manual rebuilding, the model was inspected with the program FRODO (Jones, 1985) and compared to unaveraged and 3-fold averaged $2F_{obsd} - F_{calcd}$ and $F_{obsd} - F_{calcd}$ electron density maps calculated with software from Bricogne (1976). In addition to electron density maps derived from uncomplexed protein, we also inspected maps derived from the 9-amino-9-deoxy-Neu5Acα2Me complex; data from this complex were collected on a multiwire area detector and thus had a better resolution limit (Table III) and superior merging statistics relative to the X-31 film data (Table II and Wilson et al. (1981)). Particular attention was given to main chain segments that had unusual geometry (Ramachandran & Sasiskharan, 1968) and protein side chains that had uncommon torsional configurations (Ponder & Richards, 1987; McGregor et al., 1987). These qualities were evaluated in part with the programs GEOM (written by G. H. Cohen) and O (Jones, 1991). The refined structure of X-31 BHA was used as a starting model for the refinement of the X-31 + 9-amino-9-deoxy-Neu5Acα2Me complex, during which 72 water molecules were added. None of the water molecules is located in the primary sialic acid binding site, although one is located in the second ligand binding site previously described (Sauter et al., 1992). Since an $F^{X\text{-}31+9\text{-}amino}_{obsd} - F^{X\text{-}31}_{obsd}$ electron density map showed no changes in the protein structure, this protein + water model was used in turn as the starting point for the remaining refinements. Empirical energy parameters for ligand molecules were based on those included in the X-PLOR package for α-sialic acid and hexose sugars. Parameters for synthetic derivatives of sialic acid were chosen by analogy to existing parameters, and although the resulting force field was approximate, it was adequate for refining ligand models against 3 Å resolution crystallographic data. During refinement, ligand occupancies were adjusted so that the average *B* value for atoms in the sialic acid ring would be similar to the *B* values of the protein side chains touching the ligand.

BINDING AFFINITIES OF SIALIC ACID DERIVATIVES

Shift and Broadening of Sialoside NMR Resonances in the Presence of Hemagglutinin. The dissociation constants for the interaction of sialic acids with BHA were determined by analyzing the concentration-dependent shift and broadening of the NMR resonances of these sialic acids in the presence of BHA (Sauter et al., 1989). These results are summarized in Table I. As observed by Sauter et al. (1989), all of the derivatives for which binding was detected showed an upfield shift in the resonance of the *N*-acetyl methyl protons. In the case of the *N*-propionyl derivative, both the methyl and the methylene resonances of the *N*-propionyl group are shifted

upfield. The apparent bound upfield shifts of the *N*-acyl resonances ($\Delta\delta_{Bapp}$) were calculated and ranged from 0.9 to 2.6 ppm, consistent with a common orientation of these protons over the indole of Trp-153. This upfield shift is all the more striking since no significant, concentration-dependent upfield shift was observed for any other resonance. However, many resonances, including the *N*-acetyl methyl, were broadened in the presence of BHA, and in many cases the concentration-dependent broadening of these resonances was also used to compute dissociation constants. Considering the variation in dissociation values derived from multiple resonances and from duplicate experiments, we estimate the accuracy of the dissociation constants to be ±20%.

Affinity of Modified Sialic Acids for X-31 BHA. The sialosides examined in this study are all derivatives of Neu5Acα2Me where one position has been modified. Thus, they serve as probes of the role of these positions in the interaction between sialic acid and BHA.

Consistent with previous observations that the axial carboxylate of sialic acids is critical for effective binding to BHA (Sauter et al., 1989; Pritchett, 1987; Pritchett et al., 1987), no binding was detected with the amide of Neu5Acα2Me.

Replacement of the α-*O*-methyl glycoside with an α-*O*-(4′-benzylamidocarboxybutyl) group produced the most tightly bound compound we tested. Recent crystallographic studies (Sauter et al., 1992) show that this sialoside binds to two sites on BHA. Since only the first site has the *N*-acetyl methyl located such that it will experience a large upfield shift upon binding, the *N*-acetyl shift data will reflect only the affinity for this site. Analysis of the shift of the *N*-acetyl group gave a K_D value of 1.4 mM, while the dissociation constants obtained by analysis of the line broadening of four resonances (*N*-acetyl, H_{3eq}, benzyl methylene, and 4′-methylene) ranged from 0.6 to 0.9 mM.

Sauter et al. (1989) previously showed that addition of an acetyl group at the 4-position has only a minor affect on the affinity of the sialic acid for BHA. In this study we observe that even a large phenylpropionyl substituent at the 4-position has little affect on binding affinity. The resonances of the methylene protons of the phenylpropionyl group are somewhat broadened in the presence of BHA, but not the resonances of the phenyl protons.

At the 5-position, the propionyl derivative binds with similar affinity to the corresponding acetyl derivative, and as noted above, both the methyl and methylene resonances show large upfield chemical shifts. In contrast, no concentration-dependent change in the NMR spectrum is observed for the 5-azido derivative or the large benzyloxycarbonyl derivative. By assuming that these sialosides would show broadening of their NMR resonances similar to those observed for other sialosides upon binding, we calculated lower limits on the values of the dissociation constants (Table I). These lower limits are lower than those calculated for compounds containing *N*-acetyl groups since chemical shift changes in the *N*-acetyl methyl resonance are a more sensitive indicator of binding than changes in line widths.

In contrast to the dramatic loss of affinity observed upon acetylating the 7-hydroxyl (Sauter et al., 1989; see Table I), removal of the hydroxyl at the 7-position resulted in only a 2-fold reduction in affinity. The apparent bound chemical shift change ($\Delta\delta_{Bapp}$) of the *N*-acetyl methyl resonance is 2.6 ppm, the largest so far observed for any sialoside binding to BHA.

In initial binding studies using a protein concentration of 29 μM, the *N*-acetyl methyl resonance of 9-amino-9-deoxy-Neu5Acα2Me showed a significant concentration-dependent shift. The relatively weak binding (K_D = 22 mM), and the relatively small apparent bound chemical shift (1.0 ppm, the smallest of any *N*-acetyl methyl group so far observed), made it necessary to use a higher protein concentration (86 μM) in order to obtain more precise results. At a relatively high concentration of BHA (58 μM), a very small upfield shift in the *N*-acetyl resonance of 9-*O*-acetyl-Neu5Acα2Me was observed. Whether this is a real indication of binding or simply an experimental artifact is difficult to judge since the changes in chemical shift observed (<0.0004 ppm) are similar to the digital resolution (approximately 0.0002 ppm) used in the experiment. Nevertheless, if we assume that this compound binds with an apparent bound chemical shift change similar to that observed for 9-amino-9-deoxy-Neu5Acα2Me, we calculate that the dissociation constant must be greater than 100 mM.

Change in Affinity Resulting from Mutating Gly-135 to Arg. Residue 135 of HA1 is located near the sialic acid binding site of hemagglutinin, and mutation of this residue from Gly to Arg results in an altered ability to agglutinate periodate-treated cells (Underwood et al., 1987). Neu5Acα2Me, (α2–6)sialyllactose, and (α2–3)sialyllactose all bind more weakly to the Arg-containing variant by factors of 1.9, 1.8, and 1.3, respectively (Table I). However, the apparent bound chemical shift changes ($\Delta\delta_{Bapp}$) for the *N*-acetyl methyl resonances are similar in each variant.

STEREOCHEMISTRY OF BOUND LIGANDS

Quality of the Difference Electron Density Maps. The previously reported model of sialic acid interacting with the primary ligand binding site of hemagglutinin (Weis et al., 1988) is now confirmed by five additional difference electron density maps of BHA complexed with sialic acid derivatives (Table III). Figure 2a,b shows a typical 3 Å resolution map, in which the electron density peak corresponding to 4-*O*-acetyl-Neu5Acα2Me has clear protrusions locating the carboxylate, 4-*O*-acetyl, acetamido, and glyceryl groups of the ligand. Together, these features unambiguously establish the ligand's orientation in the binding pocket. Additional bumps corresponding to the carbonyl and 7-hydroxyl oxygens (Figure 2b) suggest that the acetamido and glyceryl groups adopt the same rotamer conformations as seen in small-molecule crystal structures of β-Neu5Ac (Flippen, 1973) and its corresponding methyl ester (O'Connell, 1973). Although the density contains no clear bumps for the carboxylate oxygens, the carboxylate protrusion is slightly flattened, suggesting the rotational conformation shown in Figure 2. The difference electron density maps were of sufficient quality to detect a change of as few as three non-hydrogen atoms. This is illustrated by comparing the large protrusion corresponding to the 4-*O*-acetyl group in the difference density for 4-*O*-acetyl-Neu5Acα2Me (Figure 2a) with the distinctly smaller bump corresponding to the 4-hydroxyl group in the density for Neu5Acα2Me (Figure 2c).

Interactions between Protein and Sialic Acid. With the exception of 9-amino-9-deoxy-Neu5Ac (discussed below), all of the ligands studied had sialic acid moieties bound to positions on the protein surface that were identical within experimental error. This was observed whether or not the protein contained a Gly or an Arg residue at position 135 next to the binding site. The common location of sialic acid is depicted in Figure 3, a schematic diagram showing all of the protein residues near (α2–3)sialyllactose and all of the potential hydrogen bonds it forms with protein. Hydrogen bonds involving the

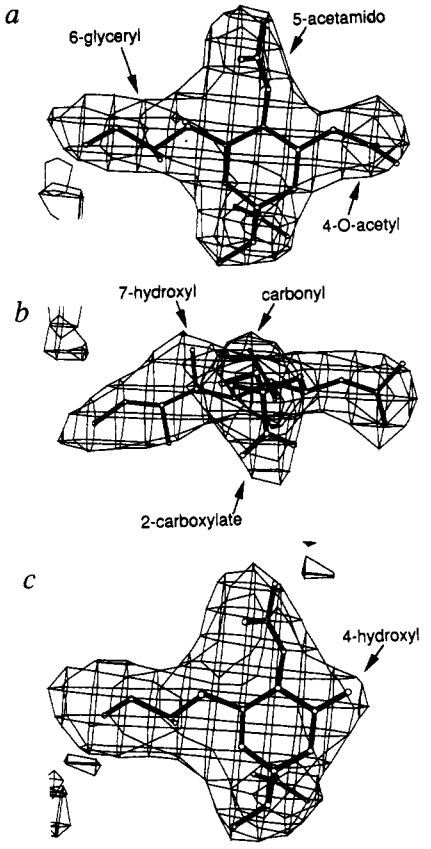

FIGURE 2: Electron density maps showing ligand in the first binding site of hemagglutinin. (a) Difference electron density map calculated with coefficients ($F_{obsd}^{X\text{-}31\ BHA + 4\text{-}O\text{-}acetyl\text{-}Neu5Ac\alpha2Me} - F_{obsd}^{X\text{-}31\ BHA})\Phi_{calcd}^{X\text{-}31\ BHA}$ from 10 to 3.0 Å resolution, averaged about the 3-fold axis of noncrystallographic symmetry and contoured here at $+3\sigma$ above the mean density. A refined model of 4-*O*-acetyl-Neu5Acα2Me is superimposed. (b) The same map and model, tilted 90°. (c) Difference electron density map calculated with coefficients ($F_{obsd}^{G135R\ BHA + Neu5Ac\alpha2Me} - F_{obsd}^{G135R\ BHA})\Phi_{calcd}^{G135R\ BHA}$ from 10 to 2.69 Å resolution, 3-fold averaged, and contoured here at $+3\sigma$. A refined model of Neu5Acα2Me is superimposed. Plots were produced with the aid of a program written by D. Freymann.

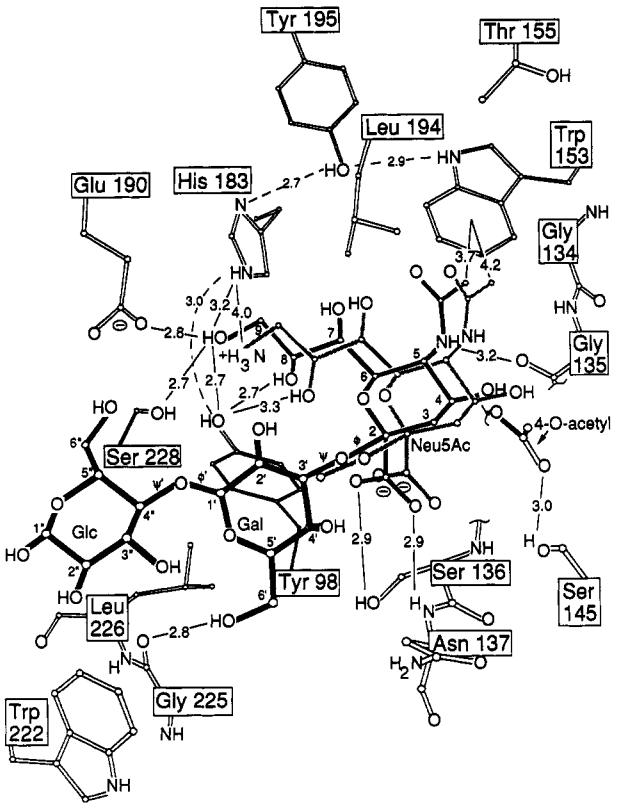

FIGURE 3: Schematic diagram of the first sialoside binding site of X-31 hemagglutinin. (α2–3)Sialyllactose is shown in black. White bonds show all protein side chains and main chain segments within 4.3 Å of (α2–3)sialyllactose. [Although Tyr-195 is more distant, it is shown to indicate its participation in a hydrogen-bond network involving residues 153, 195, 183, and 98 (dashed lines).] Intermolecular contacts between polar atoms of protein and (α2–3)-sialyllactose are listed if the contact distance is <3.4 Å; also given is the distance between the *N*-acetyl methyl group and the center of the six-membered ring of Trp-153. The shifted position of 9-amino-9-deoxy-Neu5Acα2Me is shown in gray, and contact distances are given when they differ from those for (α2–3)sialyllactose by more than 0.35 Å, the approximate coordinate error (Weis et al., 1990a). A provisional model (see text) of the 4-*O*-acetyl group of 4-*O*-acetyl-Neu5Acα2Me is depicted. Distances are in angstroms.

Neu5Ac residue include two bonds received by the carboxylate group from Ser-136 and the main chain amide of Asn-137, one donated by the acetamido nitrogen to the main chain carbonyl at Gly-135, one formed between the 8-hydroxyl and the hydroxyl of Tyr-98, and four between the 9-hydroxyl and Tyr-98, His-183, Glu-190, and Ser-228. Several difference electron density maps showed peaks in the vicinity of the binding site, suggesting that the protein may experience minor structural changes upon ligand binding (data not shown); however, these features were not consistently observed in all difference maps, nor did crystallographic refinement produce significant conformational shifts.

The Lactose Group of (α2–3)Sialyllactose. In earlier experiments, a complex between BHA and a mixture of (α2–3)- and (α2–6)sialyllactose isomers produced data showing the position of the bound Neu5Ac groups, but not of the lactose moieties (Weis et al., 1988). In the experiment presented here, the position of the Neu5Ac group of (α2–3)sialyllactose is confirmed by the difference electron density shown in Figure 4, which possesses characteristic protrusions corresponding to the ring substituents of Neu5Ac. Moreover, the electron density extends the previous results by showing the location of the lactose group. A flattened globule of electron density extending from the Neu5Ac position is large enough to accommodate the galactose ring, and a protrusion from this globule is interpreted here as corresponding to the C6′ exocyclic carbon (Figure 4). This interpretation suggests that the 6-hydroxyl of galactose may form a hydrogen bond with the carbonyl group of Gly-225 (Figure 3). A second protrusion in the density is interpreted here as corresponding to the O1′ oxygen of galactose. There is no ambiguity in deciding which protrusion corresponds to the C6′ atom and which corresponds to the O1′ atom. The glycosidic linkage joining the Neu5Ac to galactose contains only two dihedral rotational degrees of freedom, ϕ ($C1^{Neu5Ac}$–$C2^{Neu5Ac}$–$O2^{Neu5Ac}$–$C3^{Gal}$) and ψ ($C2^{Neu5Ac}$–$O2^{Neu5Ac}$–$C3^{Gal}$–$H3^{Gal}$), and the model will fit the density only with a single combination of these torsion angles. The ϕ,ψ values in the refined model (–63°,–7°) are similar to those found for the second (α2–3)sialyllactose binding site of BHA (–59°,15°; Sauter et al., 1992) and are also similar to those observed in complexes between (α2–3)sialyllactose and wheat germ agglutinin (Wright, 1990), where ϕ ranged from –72° to –65° and ψ ranged from –12° to 8°. The results cannot be compared with the uncomplexed conformation of the Neu5Ac(α2–3)Gal glycosidic bond, since no consensus exists about the configuration of the bond in solution. Although ^1H–^1H NOEs have been observed in sialyl oligosaccharides, sialyl glycolipids and sialyl glycopeptides, it has been difficult to draw structural conclusions from those data in view of the theoretical prediction that multiple torsional

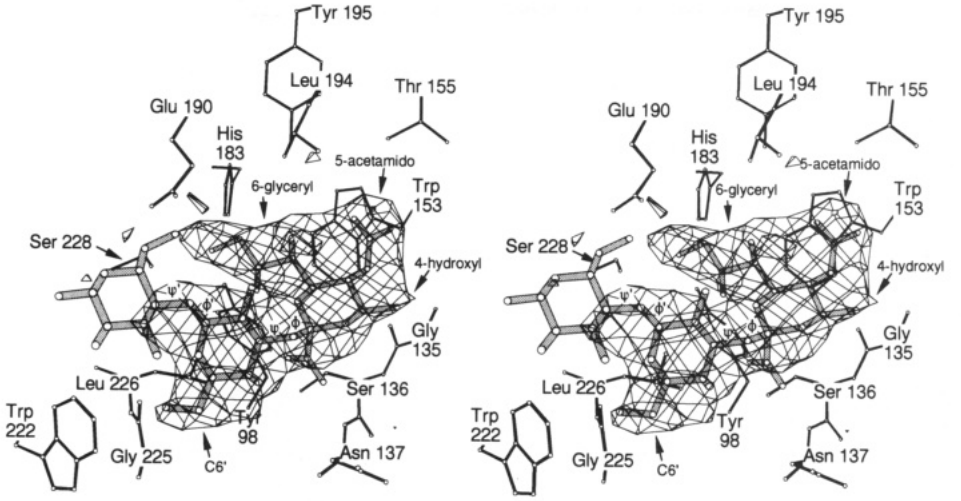

FIGURE 4: Stereoview of a difference electron density map showing the location of (α2–3)sialyllactose in the first binding site of hemagglutinin. The 3-fold averaged map was calculated with coefficients $(F_{obsd}^{X\text{-}31\ BHA + (\alpha 2\text{-}3)sialyllactose} - F_{obsd}^{X\text{-}31\ BHA})\Phi_{calcd}^{X\text{-}31\ BHA}$ from 10 to 3.0 Å resolution and contoured here at $+3\sigma$ above the mean density. A refined model is superimposed, showing the protein in black and the ligand in gray.

conformations are energetically possible (Sabesan et al., 1984; Breg et al., 1989; Poppe et al., 1989; Scarsdale et al., 1990; Sabesan et al., 1991a). The $F_{obsd} - F_{obsd}$ density peak for (α2–3)sialyllactose (Figure 4) is only large enough to cover the C3″ and C4″ carbons of the glucopyranose ring, suggesting that the glucose is partly disordered. However, it is clear from hard sphere model calculations that the Gal(β1–4)Glc glycosidic bond present in the lactose group has limited conformational freedom about the torsion angles ϕ' ($H1^{Gal}$–$C1^{Gal}$–$O1^{Gal}$–$C4^{Glc}$) and ψ' ($C1^{Gal}$–$O1^{Gal}$–$C4^{Glc}$–$H4^{Glc}$) (Rees & Skerrett, 1968). This has been confirmed by crystal structures of small molecules containing (β1–4) linkages, in which ϕ' ranges from 25° to 52° and ψ' ranges from –48° to –8° (Chu & Jeffrey, 1967; Ham & Williams, 1969; Fries et al., 1971; Bugg, 1973; Cook & Bugg, 1973; Hirotsu & Shimada, 1974; Longchambon et al., 1981), and by ^{13}C–^{1}H J couplings of methyl β-lactoside, which suggest that the ϕ',ψ' angles take on the values 40°,15° (Hayes et al., 1982). Considering the limited flexibility of the (β1–4) linkage, the glucose residue has been included in the refined model shown in Figure 4 with ϕ',ψ' values 60°,–14°. Despite its inclusion, several factors limit the usefulness of the glucose model. First, a $2F_{obsd} - F_{calcd}$ map contains electron density for only the C2″, C3″, C4″, and C5″ carbons of glucose (not shown). Second, the average B value for atoms in the glucose ring (66 Å^2) is significantly higher than those for the galactose (51 Å^2) and Neu5Ac (39 Å^2) residues. Finally, a calculation of the surface[3] accessible to a probe of radius 1.4 Å indicates that only 33% (82 Å^2) of the glucose surface is buried in the complex, compared to 45% (69 Å^2) of the galactose surface and 77% (300 Å^2) of the Neu5Ac surface. All of these factors are consistent with NMR line broadening data, suggesting that the lactose portion of the bound ligand is more mobile than the sialic acid portion (Sauter et al., 1989).

The Acetyl Side Chain of 4-O-Acetyl-Neu5Acα2Me. Even though the 4-*O*-acetyl group of 4-*O*-acetyl-Neu5Acα2Me is observed in a difference electron density map (Figure 2a), the density is not detailed enough to distinguish the positions of the methyl carbon and the carbonyl oxygen, nor are there stereochemical reasons to conclude that the acetyl group adopts one particular rotational conformation. It is possible to build models which bring either the methyl carbon or the carbonyl oxygen to within 3 Å of the hydroxyl group of Ser-145; the latter possibility suggests that the carbonyl oxygen may receive a hydrogen bond from Ser-145. However, both the acetyl group and the serine side chain are highly solvent accessible and possess higher B factors than the surrounding atoms. A hydrogen bond between them is likely to be weak, since it would exchange with hydrogen bonds to the solvent. Figure 3 shows a provisional model where the acetyl torsional angles are set to –172° (C5–C4–O4–$C^{carbonyl}$) and –67° (C4–O4–$C^{carbonyl}$–$O^{carbonyl}$).

The Glycosidic Side Chain of Neu5Acα2Bac. A difference electron density map (Figure 5) clearly shows that the sialic acid group of Neu5Acα2Bac binds to the protein in an orientation nearly identical to that of the sialic acid groups of Neu5Acα2Me, 4-*O*-acetyl-Neu5Acα2Me, and (α2–3)-sialyllactose. It was only possible, however, to determine the position of the first carbon atom of the ligand's 2-*O*-(4′-benzylamidocarboxybutyl) side chain. Although the small difference electron density peak located in the groove between Gly-225 and Ala-138 may represent some of the remaining atoms, the peak is neither connected to the larger peak representing sialic acid nor is it large enough or shaped properly to accommodate the entire side chain. Furthermore, as the side chain contains eight dihedral rotational degrees of freedom, it was not possible to select a unique model based on stereochemical reasoning alone. We note that while Neu5Acα2Bac binds to a previously described second binding site of BHA, the electron density did not establish the side chain position in that site either (Sauter et al., 1992).

The Structural Effect of Replacing the 9-Hydroxyl Group with an Amino Group. Of the five protein–ligand complexes studied, the four containing 9-hydroxyl groups have sialic acid moieties which cluster in nearly the same position. In the refined models shown in Figure 6a, the centers of their sialic acid pyranose rings are all within 0.35 Å of each other, a distance that is approximately the experimental coordinate error (Weis et al., 1990a). But in relation to the pyranose rings of these four ligands, the pyranose ring of 9-amino-9-deoxy-Neu5Acα2Me is shifted by 0.7–0.9 Å. This result is also observed in the difference electron density maps shown in Figure 6b. The density peak corresponding to 9-amino-9-deoxy-Neu5Acα2Me (dashed lines) has typical protrusions that allow us to identify the carboxylate, 2-*O*-methyl, 4-hy-

[3] Accessible surface areas, as defined by Lee and Richards (1971), were calculated with the program ACCESS by M. D. Handschumacher and F. M. Richards.

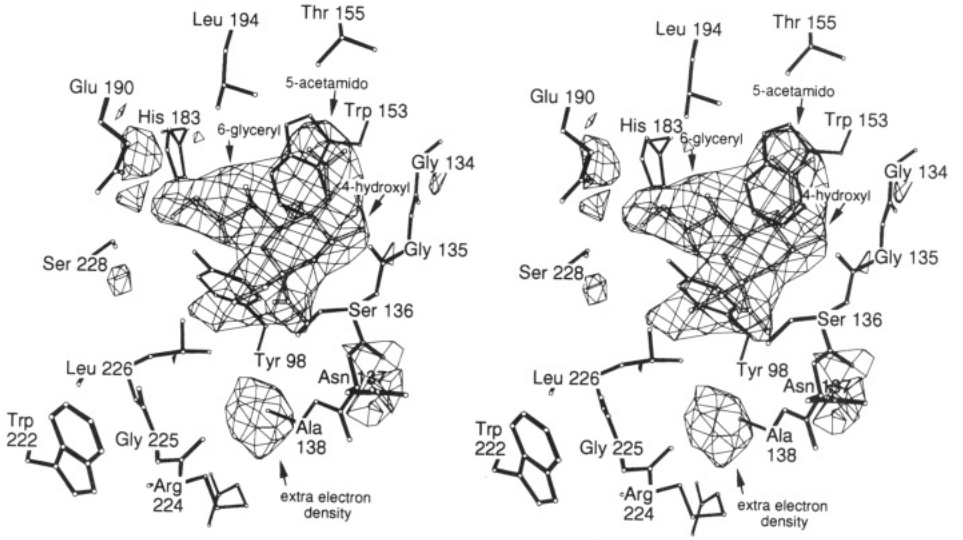

FIGURE 5: Stereoview of a difference electron density map showing the location of Neu5Acα2Bac in the first binding site of hemagglutinin. The 3-fold averaged map was calculated with coefficients $(F_{obsd}^{\text{X-31 BHA + Neu5Ac}\alpha\text{2Bac}} - F_{obsd}^{\text{X-31 BHA}})\Phi_{calcd}^{\text{X-31}}$ from 10 to 3.0 Å resolution and contoured here at $+3\sigma$ above the mean density. The map is superimposed on a refined model of protein (black) and Neu5Acα2Me (gray). The extra electron density peak suggests but does not clearly define the location of the remaining atoms of the 2-*O*-(4′-benzylamidocarboxybutyl) side chain.

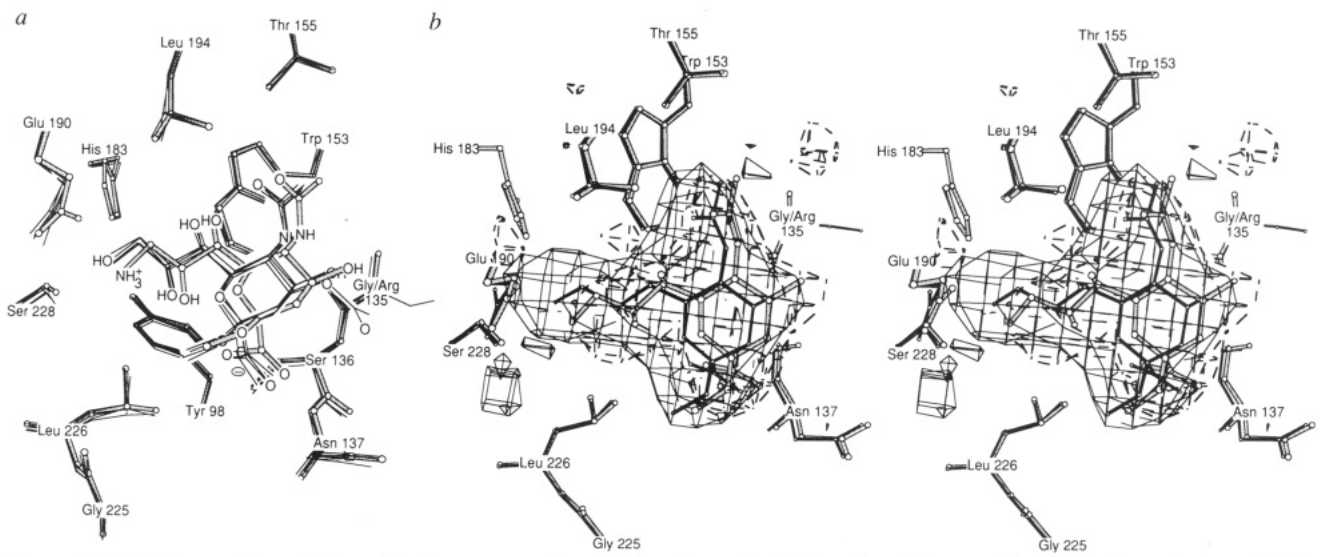

FIGURE 6: (a) Superposition of five refined structures, showing the change in sialic acid position resulting from the replacement of the 9-hydroxyl group with an amino group. Thin black bonds: BHA complexed with 4-*O*-acetyl-Neu5Acα2Me, (α2–3)sialyllactose, Neu5Acα2Bac, and Neu5Acα2Me. Thick grey bonds: BHA complexed with 9-amino-9-deoxy-Neu5Acα2Me. (b) Stereoview from a different vantage point of two difference electron density maps, calculated with coefficients $(F_{obsd}^{\text{G135R BHA + Neu5Ac}\alpha\text{2Me}} - F_{obsd}^{\text{G135R BHA}})\Phi_{calcd}^{\text{G135R BHA}}$ (solid lines; 10 to 2.69 Å resolution) and $(F_{obsd}^{\text{X-31 BHA + 9-amino-9-deoxy-Neu5Ac}\alpha\text{2Me}} - F_{obsd}^{\text{X-31 BHA}})\Phi_{calcd}^{\text{X-31 BHA}}$ (dashed lines; 10 to 3.0 Å resolution), 3-fold averaged and contoured here at $+3\sigma$ above the mean density. The maps are superimposed on refined models of BHA complexed with Neu5Acα2Me (black) and 9-amino-9-deoxy-Neu5Acα2Me (gray).

droxyl, acetamido, and amino diol groups of the molecule, yet the entire peak is shifted with respect to the Neu5Acα2Me density (solid lines). An inspection of the refined model suggests that the positional shift could be the result of electrostatic repulsion between the introduced amino group and His-183 (Figure 3). Neu5Ac ligands containing a 9-hydroxyl group presumably accept a hydrogen bond from the $N^{\epsilon 2}$ atom of histidine, which is normally located about 3.2 Å away and is likely to be protonated. When the positively charged amino group is introduced, the group shifts to a position 4.0 Å from the $N^{\epsilon 2}$ atom, while it retains close proximity to the carboxylate group of Glu-190 and the hydroxyl groups of Ser-228 and Tyr-98. Several other interactions between ligand and protein are also preserved when the amino group is introduced. For example, the ligand's carboxylate group still receives hydrogen bonds from the hydroxyl group of Ser-136 and the main chain amide group of Asn-137. Also, the acetamido nitrogen still donates a hydrogen bond to the carboxylate oxygen of Gly-135. Even though the ligand shifts in relation to His-183, these interactions are maintained by small conformational changes in the protein (changes that are too small to be identified as significant at 3 Å resolution). However, other interactions are not maintained. In particular, the 8-hydroxyl shifts from 2.7 to 3.3 Å away from the Tyr-98 hydroxyl, and the acetamido methyl group shifts from 3.7 to 4.2 Å away from the center of the six-membered ring of Trp-153. Tyr-98 and Trp-153 apparently cannot compensate for the shift in the ligand's position, for they are held fixed in relation to His-183 by a hydrogen-bond network extending from Trp-153 through Tyr-195 and His-183 and finally to Tyr-98. The fixed relationship of these four residues was previously shown by a hemagglutinin structure containing

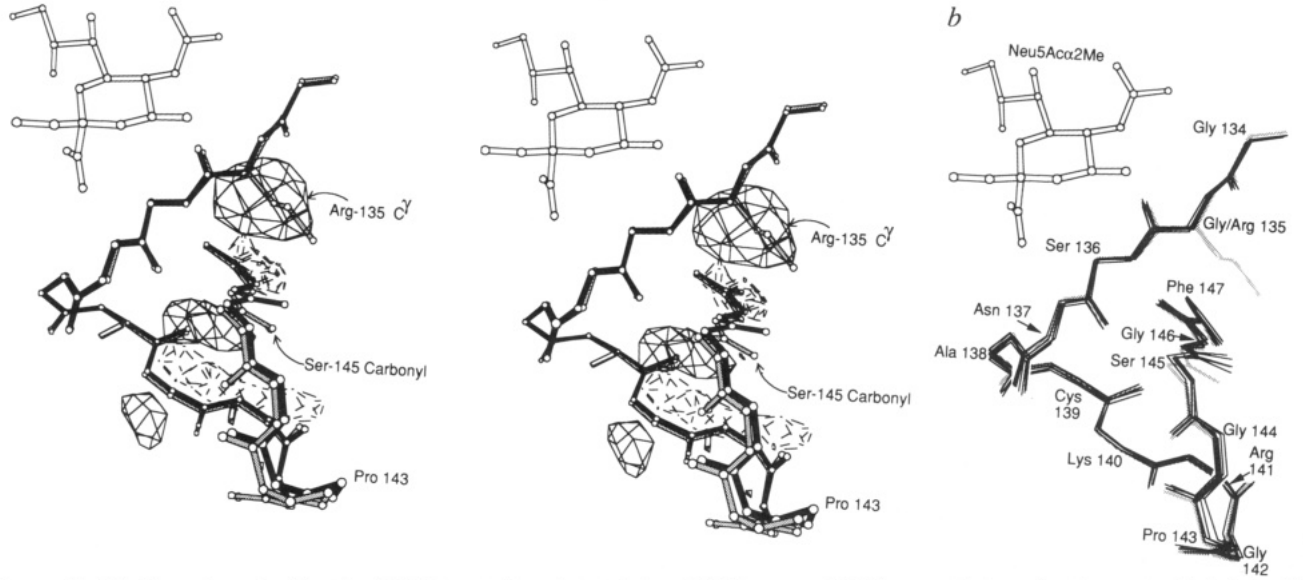

FIGURE 7: (a) Stereoview showing the G135R mutation, detected in a 3-fold averaged difference electron density map calculated with coefficients $(F_{obsd}^{G135R\ BHA} - F_{obsd}^{X\text{-}31\ BHA})\Phi_{calcd}^{X\text{-}31\ BHA}$ from the 10 to 3.0 Å resolution. The map is contoured here at $+4.5\sigma$ (solid lines) and -4.5σ (dashed lines) away from the mean density. The superimposed models show the main chain atoms of HA1 residues 134–147 (black, X-31 BHA; gray, G135R BHA). The location of the ligand binding site is also indicated. (b) Superposition of the main chain atoms of the seven refined structures listed in Table III (black, five structures with X-31 BHA; gray, two structures with G135R BHA).

the nearby mutation L226Q (Weis et al., 1988). Although the four residues are perturbed by the mutation, they shift as a block to retain their interresidue spacings.

The Structural Effect of Mutating Gly-135 to Arg. An electron density map calculated with coefficients $F_{obsd}^{G135R} - F_{obsd}^{X\text{-}31}$) gives a peak in the expected position of an L-amino acid side chain at residue 135. When an arginine is modeled into this peak as an extended chain, there is enough density to cover the side chain out to C^{γ} (Figure 7a). The absence of additional electron density suggests that the remainder of the side chain is disordered, consistent with its position on the protein surface and its accessibility to solvent. Besides its interactions with the solvent, the guanidinium group of the side chain could potentially form a hydrogen bond to the carbonyl group of Ser-145. This, however, is based solely on interactive model building; a refined structure gives *B* factors for the guanidinium group above 60 Å^2, so that its position cannot be established from the data. The G135R substitution causes only minor changes in the remainder of the protein structure. Figure 7a shows a series of small negative and positive peaks in the difference electron density, suggesting shifts in the peptide loop from residues 140 to 145. The magnitude of these shifts is illustrated in Figure 7b, which compares all seven refined structures listed in Table III. The most significant shift is that of the carbonyl oxygen of Ser-145, which moves between 0.6 and 1.1 Å relative to its position in X-31 structures, apparently allowing the peptide loop to accommodate the new arginine side chain. The introduction of an arginine at position 135 causes no change in the position of bound Neu5Ac. This is seen in Figure 6a, which shows that the Neu5Ac moieties of three compounds [4-*O*-acetyl-Neu5Acα2Me, (α2–3)sialyllactose, and Neu5Acα2Bac] complexed with X-31 BHA occupy the same position as Neu5Acα2Me complexed with G135R BHA.

DISCUSSION

The NMR experiments presented here (Table I) add to the list of sialic acid analogs whose binding affinities to X-31 hemagglutinin have been evaluated. Figure 8a summarizes our current knowledge of how the ligand affinity is changed by functional substitutions at six positions of the fundamental α-sialoside, Neu5Acα2Me. Three-dimensional structural information from five BHA–sialoside complexes (Tables II and III) allows us to interpret the binding data in terms of the specific interactions that each functional group makes with the first binding site (a second site is discussed in Sauter et al. (1992)).

Substituent R_1 of Neu5Acα2Me is the axial carboxylate group attached to the anomeric carbon. The difference electron density maps presented here (Figures 2, 4, 5, and 6) show the carboxylate group much more clearly than previous studies (Weis et al., 1988) and confirm that one carboxylate oxygen receives a hydrogen bond from the hydroxyl group of Ser-136, while the other receives a hydrogen bond from the main chain amide group at Asn-137. Modification of the R_1 group is known to abolish or reduce ligand binding. X-31 hemagglutinin does not bind to compounds in which the carboxylate group is switched to the equatorial R_2 position, and the axial R_1 substituent is replaced by either an *O*-methyl group (Neu5Acβ2Me; Pritchett, 1987; Sauter, 1989; Kelm et al., 1992) or a hydrogen atom (2-deoxy-2H_{ax}-Neu5Ac; Kelm et al., 1992). In these compounds, the equatorial positioning of the carboxylate should not by itself abolish binding, since R_2 points toward the solvent without touching the protein directly. Instead, binding is probably abolished by the absence of any atoms in the R_1 position that could form hydrogen bonds with residues 136 and 137. A less drastic change in R_1 is the conversion of the acid to either the methyl or ethyl esters, reducing ligand affinity by a factor of 10 or more as measured by inhibition of viral attachment to cells (Pritchett, 1987; Kelm et al., 1992). Although these compounds can still receive one hydrogen bond through the ester carbonyl oxygen, their reduced affinities may be explained by (1) the loss of the second hydrogen bond and/or (2) the increased volume occupied by the methyl or ethyl groups that possibly makes the R_1 group too bulky to fit in the space that it occupies in

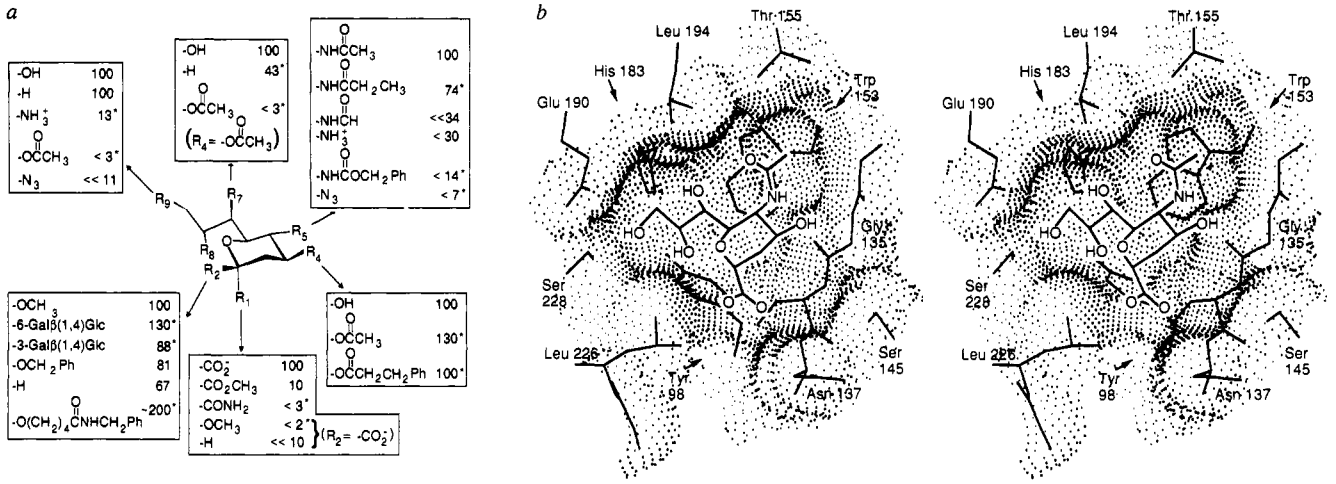

FIGURE 8: (a) Effect of functional modifications on the binding of sialosides to X-31 hemagglutinin. Binding of each ligand analog is expressed as a relative affinity, where Neu5Acα2Me = 100. Values determined by NMR are denoted by asterisks (*). References for other experiments are given in the text. (b) Schematic drawing of an α-sialoside bound to X-31 hemagglutinin, based on the crystal structure of BHA complexed with (α2–3)sialyllactose. The molecular surface shown is the contact surface for a probe of radius 1.4 Å. Dense points represent the surface buried by the Neu5Ac residue upon ligand binding, while sparse points represent the surrounding area.

the known crystal structures (Figure 8b). We replaced the carboxylate with an amide, a group that has approximately the same volume as the carboxylate, but where one of the hydrogen-bond-accepting atoms is replaced by a hydrogen-bond donor. No binding to hemagglutinin was observed (Table I), reinforcing the idea that binding requires the ligand to accept hydrogen bonds from both Ser-136 and Asn-137. It remains to be seen what would happen if the carboxylate were replaced with methyl ketone ($COCH_3$) or 2-propene ($C(CH_3)=CH_2$) groups, which would also be isosteric, but in which one or both hydrogen-bond-accepting atoms are replaced with carbons.

Sialic acid is attached to cell-surface oligosaccharides through several types of glycosidic linkages (reviewed by Paulson, 1985). Mutations at position 226 of HA1 alter the binding specificity of hemagglutinin for (α2–3) and (α2–6) linkages (Rogers et al., 1983; Pritchett, 1987; Sauter et al., 1989), suggesting that the asialo portion of the saccharide interacts in some way with the protein. However, crystallographic data, previously collected from complexes of BHA and a mixture of (α2–3)- and (α2–6)sialyllactose isomers, gave no indication of the lactose position(s) (Weis et al., 1988). We have now investigated a complex between BHA and purified (α2–3)sialyllactose that for the first time enables us to determine the lactose conformation (Figures 3 and 4). Although the lactose is relatively disordered, it can potentially donate at least one hydrogen bond to the protein from the 6-hydroxyl of galactose to the main chain carbonyl oxygen of Gly-225. Further study of BHA–oligosaccharide complexes may therefore reveal the structural basis for the ligand specificity produced by amino acid 226.

Now that we know that asialo portions of sialyl oligosaccharides can be detected crystallographically, two other aspects of oligosaccharide binding present themselves for study. First, several sialyl oligosaccharides bind very weakly to X-31 hemagglutinin for unknown reasons. The ganglioside-derived $G_{M1}OS$, for example, binds at least 12 times weaker than (α2–3)sialyllactose even though it contains the (α2–3)-sialyllactose sequence, Neu5Ac(α2–3)Gal(β1–4)Glc[4] (Sauter et al., 1989). A crystal structure might reveal unfavorable interactions that would account for its weak affinity. Second, none of the naturally occurring mono- or disialylated oligosaccharides studied so far have bound to hemagglutinin with significantly higher affinity than Neu5Acα2Me (Pritchett, 1987; Pritchett et al., 1987; Sauter et al., 1989). This suggests that, even though we can observe the asialo portion of a saccharide in a specific orientation, its interactions with the protein may not be important for the overall binding reaction. Nevertheless, we cannot rule out the possibility that future studies will discover naturally occurring saccharides where the presence of the asialo portion does increase the binding affinity.

It is possible to glycosylate α-sialic acid with a variety of alcohols, making it possible to investigate whether novel *O*-glycosides can improve the binding affinity. Initial studies with $R_2 = OCH_2C_6H_5$, H, and *O*-naphthyl showed little effect (Pritchett, 1987; Pritchett et al., 1987; Kelm et al., 1992), consistent with the crystallographic result that the R_2 substituent is oriented toward solution without necessarily making any contacts with protein. More difficult to understand are recent results showing that glycosides of the form $R_2 = O(CH_2)_nCONHR'$ allow sialic acid to inhibit hemagglutination with significantly greater potency than Neu5Acα2Me: as much as 64-fold in the case where $n = 6$ and R′ is a 1-naphthylmethyl group (Toogood et al., 1991). We have studied Neu5Acα2Bac (Figure 1), the first such compound to be synthesized. NMR data indicated that the substitution of the α-*O*-methyl glycoside with a (4′-benzylamidocarboxybutyl) group increases ligand affinity for the first site by a factor of 2–4 (Table I). A difference electron density map revealed that the Neu5Ac portion of Neu5Acα2Bac binds to the protein in the usual orientation. In addition, although an extra density peak in the groove between Ala-138 and Gly-225 (Figure 5) suggested the location of the glycosidic side chain, the peak was too small to accommodate a model of the side chain. Therefore, the structural basis for the improved affinity given by this class of glycosides is not yet clear.

Substituent R_4 of Neu5Acα2Me is an equatorial hydroxyl group, but R_4 is an *O*-acetyl group in a fraction of sialic acid isolated from equine species (Schauer, 1982). Our previously determined structure of the BHA–sialyllactose complex (Weis et al., 1988) suggested that the R_4 substituent sticks out of

[4] Its full sequence is Gal(β1–3)GalNAc(β1–4)[Neu5Ac(α2–3)]Gal(β1–4)Glc.

the binding site toward solution, without making direct contact with the protein. It was therefore not surprising when NMR experiments showed that the 4-*O*-acetyl group does not significantly change the ligand affinity (Sauter et al., 1989). This result suggested that neither the 4-hydroxyl nor the 4-*O*-acetyl group contributes significantly to the binding strength and that the affinity would remain unchanged even if the R_4 substituent were replaced by a hydrogen. The conclusion that the acetyl group does not contact the protein was supported by NMR spectra, showing that the presence of protein does not cause any line broadening in the 4-*O*-acetyl methyl resonance. The X-ray structure (Figure 2) confirms that the acetyl group is highly solvent accessible. Crystallographic refinement places one of the atoms of the acetyl group (either the methyl carbon or the carbonyl oxygen) within 3.3 Å of the carbonyl oxygen of Gly-135 and within 3.0 Å of the hydroxyl group of Ser-145, but since the acetyl atoms have high *B* values, these are not expected to be strong contacts. We synthesized the 4-*O*-phenylpropionyl derivative of Neu5Acα2Me in the hope that the additional atoms in the *O*-acyl chain would form specific interactions with the protein. However, an NMR experiment shows that even this substitution does not alter the ligand affinity (Table I).

One property of 4-*O*-acetyl-Neu5Acα glycosides is that they are partially resistant to the action of influenza neuraminidase, which normally cleaves the α-glycosidic bond (Schauer, 1982). Resistance to neuraminidase would be an important property for any inhibitor designed to interfere with viral function. It is possible that the addition of bulkier substituents at the 4-position might confer complete resistance to neuraminidase without affecting the affinity to hemagglutinin. An alternative would be to incorporate a carbon–glycoside bond into the inhibitor, as has recently been done with the synthesis of a compound where $R_1 = CH_2CH{=}CH_2$ (Nagy & Bednarski, 1991).

The usual R_5 substituent is the *N*-acetyl group, which contacts the indole ring of Trp-153 and thus experiences a significant ring current shift, as observed in ^1H NMR spectra. Hemagglutination studies indicate that, if a hydroxyl group is added to the side chain to form *N*-glycolylneuraminic acid ($R_5 = NHCOCH_2OH$), the resulting glycosides do not act as cell-surface receptors for X-31 virus (Higa et al., 1985). This is puzzling, since the three-dimensional structure suggests that there is room for at least one more non-hydrogen atom in the pocket formed by Trp-153 and Thr-155 (Figure 8b). It is possible that binding of the *N*-glycolyl chain to the protein would be electrostatically unfavorable. In the hope that an extra methyl group might increase the affinity by making additional hydrophobic interactions with the indole ring, we synthesized the 5-*N*-propionyl analog ($R_5 = NHCOCH_2CH_3$) of Neu5Acα2Me. NMR spectra showed that both the methylene and methyl protons of the *N*-propionyl ethyl group experience large upfield chemical shifts in the presence of protein (Table I), suggesting that the ethyl group binds above the indole ring as expected. However, the dissociation constant is virtually the same as that of Neu5Acα2Me. We note that *N*-glycolylneuraminic acid does act as a cell-surface receptor for viruses containing tyrosine instead of threonine at position 155 (Higa et al., 1985). However, a structural explanation awaits further experiments to determine the tyrosine position in these mutants.

Other alterations at the 5-position have been made, but those tested have produced analogs that bind much more weakly (if at all) to hemagglutinin. Our NMR experiments failed to detect any binding (Table I) between X-31 BHA and 5-*N*-(benzyloxycarbonyl)-Neuα2Me ($R_5 = NHCOOCH_2C_6H_5$) or 5-azido-5-deamino-Neuα2Me ($R_5 = N_3$). In addition, little or no inhibition of the attachment of X-31 virus to erythrocytes was observed with an α-sialoside of neuraminic acid ($R_5 = NH_3^+$) or with the corresponding *N*-formyl, *N*-3-carboxypropanoyl, *N*-trifluoroacetyl, or *N*-bromoacetyl derivatives (Pritchett, 1987; Kelm et al., 1992). Since these alterations did not produce compounds with enhanced affinity for hemagglutinin, future experiments should systematically screen additional R_5 analogs. The *N*-butyryl ($R_5 = NHCOCH_2CH_2CH_3$) and *N*-cyclopropyl ($R_5 = NHCO\text{-}C_3H_5$) analogs would answer the question of whether longer and bulkier side chains would fit in the binding site. The urea ($R_5 = NHCONH_2$) analog would test whether the amide group could enhance binding by forming a hydrogen bond with the aromatic face of the indole ring of Trp-153, as has been suggested for other systems (Perutz et al., 1986; Levitt & Perutz, 1988).

One facet of the hemagglutinin–sialic acid complex that still needs to be adequately explored is the proximity of two polar atoms to the hydrophobic side chain of Leu-194. Leucine $C^{\delta 2}$ is the closest protein atom to both the carbonyl oxygen of R_5 (3.3 Å away) and the hydroxyl oxygen of R_7 (3.9 Å away). Neither ligand atom makes hydrogen bonds to the protein. In a small-molecule crystal structure of β-Neu5Ac methyl ester, the 7-hydroxyl group donates an intramolecular hydrogen bond to the carbonyl oxygen (O'Connell, 1973), but this hydrogen bond is absent in a crystal structure of β-Neu5Ac (Flippen, 1973). In order to assess whether such a hydrogen bond is necessary for ligand binding to hemagglutinin, we synthesized the 7-deoxy analog of Neu5Acα2Me ($R_7 = H$). An NMR experiment showed that the affinity of the resulting compound for X-31 BHA is about half that of the parent compound, indicating that an intramolecular hydrogen bond is not strictly necessary. [In contrast, Kelm et al. (1992) report that, in a series of analogs with $R_2 = H$, removal of the 7-hydroxyl group reduces inhibition of viral attachment to erythrocytes by more than 7-fold. The reason for the difference in the importance of the 7-hydroxyl in our compound compared to that studied by Kelm et al. is not known.] Our result suggests that further alterations could be made in the ligand to maximize its hydrophobic interactions with Leu-194. The R_5 substituent, for example, could be replaced by the thioamide, $NH(C{=}S)CH_3$, which would preserve the sp^2 character of the carbonyl carbon, yet decrease its polarity. The R_7 group has already been replaced by an *O*-acetyl group, an alteration which abolishes binding (Sauter et al., 1989). This is consistent with the crystal structure, which suggests that an *O*-acetyl group is too bulky to be accommodated next to Leu-194. However, smaller and more flexible substituents would fit in this space, and a suitably hydrophobic ligand analog might be discovered by trying a series of sustitutions at R_7, including CH_3, CH_2CH_3, $CH_2(CH_3)CH_3$, OCH_3, and OCH_2CH_3.

The usual substituent at the R_9 position is a hydroxyl group. The naturally occurring 9-*O*-acetyl analog fails to act as a cell-surface receptor for hemagglutination (Higa et al., 1985) and does not bind detectably to X-31 BHA by NMR (Table I). Synthetic analogs containing $R_9 = N_3$ or CN fail to inhibit viral attachment to cells (Pritchett, 1987; Kelm et al., 1992). The crystal structure suggests that these substituents may be too bulky to be accommodated next to the protein. We reasoned that an amino group at the 9-position would be nearly isosteric with the normal 9-hydroxyl and that the positively charged amino group would then be positioned to interact

favorably with the Glu-190 carboxylate. However, the resulting compound, 9-amino-9-deoxy-Neu5Acα2Me, bound with 8-fold lower affinity than the parent compound (Table I). The amino group formed a salt bridge with the Glu-190 carboxylate but moved away from the imidazolium group of His-183, causing the entire ligand to move to a slightly different position in the binding site (Figure 6). The group retained its close contact distances to the Ser-228 and Tyr-98 hydroxyls, indicating that these residues accept hydrogen bonds from the ligand. Although our structural studies with a variety of sialosides suggest potential hydrogen bonds between the 9-hydroxyl and four groups (the His-183 imidazolium, the Glu-190 carboxylate, and the Ser-228 and Tyr-98 hydroxyls), Kelm et al. (1992) report that replacing the 9-hydroxyl with a hydrogen leaves the binding affinity unchanged. This result might be explained if the hydrogen bonds between the 9-hydroxyl and the protein are not energetically optimal or if the 9-deoxy compound binds in a different conformation that compensates for the binding energy lost by the removal of the 9-hydroxyl.

A final class of ligand alterations involves the oxidation of Neu5Ac by periodate to leave an aldehyde at carbon 8 or carbon 7, followed optionally by borohydride reduction giving the C8 and C7 alcohols. Relative to Neu5Acα2Me, the C7 alcohol has a 12-fold reduced potency for inhibiting the attachment of X-31 virus to erythrocytes, while the C7 aldehyde has an even further reduced potency (Pritchett, 1987; Kelm et al., 1992). Modification of the sialyl glycoprotein fetuin led to similar effects on the virus' ability to attach to the protein (Matrosovich et al., 1991). Treatment of erythrocytes to produce the C7 aldehyde sharply reduced hemagglutination by X-31 (Underwood et al., 1987). In the same study, however, the mutation of amino acid 135 of HA1 from Gly to Arg was found to partly counteract the loss of hemagglutination ability. This was unexpected, since amino acid 135 lies on the opposite side of the binding pocket from C7 (Figure 3). In order to determine if the mutation caused some unknown change in the protein structure, we determined the structures of both the mutant protein (Figure 7) and the mutant protein complexed with Neu5Acα2Me. Neither data set revealed any structural alterations due to the amino acid substitution, so that the hemagglutination results are still unaccounted for. More research will be necessary to determine whether there are other components of the erythrocyte surface that interact with the amino acid at position 135.

The results presented here begin to show which functional substituents of sialic acid are necessary for its binding to X-31 hemagglutinin and what types of modifications will diminish its affinity. We have used the three-dimensional structure of the protein–ligand complex to decide which analogs to investigate in the search for higher affinity binding inhibitors. More analogs remain to be investigated, and their synthesis poses a significant challenge to organic chemistry.

ACKNOWLEDGMENTS

We thank David Stevens and Alan Douglas for excellent technical assistance; Greg Priebe and George Whitesides (Department of Chemistry, Harvard University) for the gift of the methyl ester of 5-*N*-(benzyloxycarbonyl)-Neuα2Me; Andreas Schrell and George Whitesides for the gift of the 5-azido-5-deamino-Neuα2Me; and Jim Mace (University of California at San Francisco) for his help with Figure 8b.

SUPPLEMENTARY MATERIAL AVAILABLE

A listing of details of the organic syntheses, including ^{1}H and ^{13}C NMR data for synthetic intermediates (13 pages). Ordering information is given on any current masthead page.

REFERENCES

Bergh, M. L. E., Koppen, P., & van den Eijnden, D. H. (1981) *Carbohyd. Res. 94*, 225–229.
Blum, M., Metcalf, P., Harrison, S. C., & Wiley, D. C. (1987) *J. Appl. Crystallogr. 20*, 235–242.
Brand, C. M., & Skehel, J. J. (1972) *Nature 238*, 145–147.
Breg, J., Kroon-Batenburg, L. M. J., Strecker, G., Montreuil, J., & Vliegenthart, J. F. G. (1989) *Eur. J. Biochem. 178*, 727–739.
Bricogne, G. (1976) *Acta Crystallogr. A32*, 832–847.
Brown, J. H. (1991) Ph.D. Thesis, Harvard University, Cambridge, MA.
Brünger, A. T. (1990) *X-PLOR Manual*, version 2.1, Yale University, New Haven, CT.
Bugg, C. E. (1973) *J. Am. Chem. Soc. 95*, 908–913.
Carroll, S. M., Higa, H. H., & Paulson, J. C. (1981) *J. Biol. Chem. 256*, 8357–8363.
Chu, S. S. C., & Jeffrey, G. A. (1968) *Acta Crystallogr. B24*, 830–838.
Cook, W. J., & Bugg, C. E. (1973) *Acta Crystallogr. B29*, 907–909.
Daniels, R. S., Douglas, A. R., Skehel, J. J., & Wiley, D. C. (1983) *J. Gen. Virol. 64*, 1657–1662.
Durbin, R. M., Burns, R., Moulai, J., Metcalf, P., Freymann, D., Blum, M., Anderson, J. E., Harrison, S. C., & Wiley, D. C. (1986) *Science 232*, 1127–1132.
Flippen, J. L. (1973) *Acta Crystallogr. B29*, 1881–1886.
Fries, D. C., Rao, S. T., & Sundaralingam, M. (1971) *Acta Crystallogr. B27*, 994–1005.
Gamian, A., Chomik, M., Laferrière, C. A., & Roy, R. (1991) *Can. J. Microbiol. 37*, 233–237.
Glick, G. D., & Knowles, J. R. (1991) *J. Am. Chem. Soc. 113*, 4701–4703.
Glick, G. D., Toogood, P. L., Wiley, D. C., Skehel, J. J., & Knowles, J. R. (1991) *J. Biol. Chem. 266*, 23660–23669.
Ham, J. T., & Williams, D. G. (1970) *Acta Crystallogr. B26*, 1373–1383.
Hayes, M. L., Serianni, A. S., & Barker, R. (1982) *Carbohydr. Res. 100*, 87–101.
Higa, H. H., Rogers, G. N., & Paulson, J. C. (1985) *Virology 144*, 279–282.
Hirotsu, K., & Shimada, A. (1974) *Bull. Chem. Soc. Jpn. 47*, 1872–1879.
Jones, T. A. (1985) *Methods Enzymol. 115*, 157–171.
Jones, T. A., Zou, J.-Y., Cowan, S. W., & Kjeldgaard, M. (1991) *Acta Crystallogr. A47*, 110–119.
Kelm, S., Paulson, J. C., Rose, U., Brossmer, R., Schmid, W., Bandgar, B. P., Schreiner, E., Hartmann, M., & Zbiral, E. (1992) *Eur. J. Biochem. 205*, 147–153.
Knossow, M., Daniels, R. S., Douglas, A. R., Skehel, J. J., & Wiley, D. C. (1984) *Nature 311*, 678–680.
Knossow, M., Lewis, M., Rees, D., Wilson, I. A., Skehel, J. J., & Wiley, D. C. (1986) *Acta Crystallogr. B42*, 627–632.
Lee, B., & Richards, F. M. (1971) *J. Mol. Biol. 55*, 379–400.
Levitt, M., & Perutz, M. F. (1988) *J. Mol. Biol. 201*, 751–754.
Longchambon, F., Ohanessian, J., Gillier-Pandraud, H., Duchet, D., Jacquinet, J.-C., & Sinaÿ, P. (1974) *Acta Crystallogr. B37*, 601–607.
Matrosovich, M. N., Mochalova, L. V., Marinina, V. P., Byramova, N. E., & Bovin, N. V. (1990) *FEBS Lett. 272*, 209–212.
Matrosovich, M. N., Gambaryan, A. S., Reizin, F. N., & Chumakov, M. P. (1991) *Virology 182*, 879–882.
McGregor, M. J., Islam, S. A., & Sternberg, M. J. E. (1987) *J. Mol. Biol. 198*, 295–310.
Nagy, J. O., & Bednarski, M. D. (1991) *Tetrahedron Lett. 32*, 3953–3956.
O'Connell, A. M. (1973) *Acta Crystallogr. B29*, 2320–2328.

Paulson, J. C. (1985) in *The Receptors* (Conn, P. M., Ed.) Vol. 2, pp 131–219, Academic, Orlando, FL.
Perutz, M. F., Fermi, G., Abraham, D. J., Poyart, C., & Bursaux, E. (1986) *J. Am. Chem. Soc. 108*, 1064–1078.
Ponder, J. W., & Richards, F. M. (1987) *J. Mol. Biol. 193*, 775–791.
Poppe, L., Dabrowski, J., von der Lieth, C.-W., Numata, M., & Ogawa, T. (1989) *Eur. J. Biochem. 180*, 337–342.
Pritchett, T. J. (1987) Ph.D. Thesis, University of California, Los Angeles.
Pritchett, T. J., Brossmer, R., Rose, U., & Paulson, J. C. (1987) *Virology 160*, 502–506.
Pritchett, T. J., & Paulson, J. C. (1989) *J. Biol. Chem. 264*, 9850–9858.
Ramachandran, G. N., & Sasiskharan, V. (1968) *Adv. Protein Chem. 23*, 283–437.
Rees, D. A., & Skerrett, R. J. (1968) *Carbohydr. Res. 7*, 334–348.
Rogers, G. N., Paulson, J. C., Daniels, R. S., Skehel, J. J., Wilson, I. A., & Wiley, D. C. (1983) *Nature 304*, 76–78.
Sabesan, S., Bock, K., & Lemieux, R. U. (1984) *Can. J. Chem. 62*, 1034–1045.
Sabesan, S., Duus, J. Ø., Fukunaga, T., Bock, K., & Ludvigsen, S. (1991a) *J. Am. Chem. Soc. 113*, 3236–3246.
Sabesan, S., Duus, J. Ø., Domaille, P., Kelm, S., & Paulson, J. C. (1991b) *J. Am. Chem. Soc. 113*, 5865–5866.
Sauter, N. K., Bednarski, M. D., Wurzburg, B. A., Hanson, J. E., Whitesides, G. M., Skehel, J. J., & Wiley, D. C. (1989) *Biochemistry 28*, 8388–8396.
Sauter, N. K. (1991) Ph.D. Thesis, Harvard University, Cambridge, MA.
Sauter, N. K., Glick, G. D., Crowther, R. L., Park, S.-J., Eisen, M. B., Skehel, J. J., Knowles, J. R., & Wiley, D. C. (1992) *Proc. Natl. Acad. Sci. U.S.A. 89*, 324–328.
Scarsdale, J. N., Prestegard, J. H., & Yu, R. K. (1990) *Biochemistry 29*, 9843–9855.
Schauer, R. (1982) *Adv. Carbohydr. Chem. 40*, 132–235.
Spaltenstein, A., & Whitesides, G. M. (1991) *J. Am. Chem. Soc. 113*, 686–687.
Still, W. C., Kahn, M., & Mitra, A. (1978) *J. Org. Chem. 43*, 2923–2925.
Suttajit, M., & Winzler, R. J. (1971) *J. Biol. Chem. 246*, 3398–3404.
Toogood, P. L., Galliker, P. K., Glick, G. D., & Knowles, J. R. (1991) *J. Med. Chem. 34*, 3138–3140.
Underwood, P. A., Skehel, J. J., & Wiley, D. C. (1987) *J. Virol. 61*, 206–208.
van der Vleugel, D. J. M., van Heeswijk, W. A. R., & Vliegenthart, J. F. G. (1982) *Carbohydr. Res. 102*, 121–130.
Verhoeyen, M., Fang, R., Min Jou, W., Devos, R., Huylebroeck, D., Saman, E., & Fiers, W. (1980) *Nature 286*, 771–776.
Weis, W. I. (1987) Ph.D. Thesis, Harvard University, Cambridge, MA.
Weis, W., Brown, J. H., Cusack, S., Paulson, S. C., Skehel, J. J., & Wiley, D. C. (1988) *Nature 333*, 426–431.
Weis, W. I., Brünger, A. T., Skehel, J. J., & Wiley, D. C. (1990a) *J. Mol. Biol. 212*, 737–761.
Weis, W. I., Cusack, S. C., Brown, J. H., Daniels, R. S., Skehel, J. J., & Wiley, D. C. (1990b) *EMBO J. 9*, 17–24.
Wiley, D. C., & Skehel, J. J. (1977) *J. Mol. Biol. 112*, 343–347.
Wiley, D. C., & Skehel, J. J. (1987) *Annu. Rev. Biochem. 56*, 365–394.
Wilson, I. A., Skehel, J. J., & Wiley, D. C. (1981) *Nature 289*, 366–373.
Wright, C. S. (1990) *J. Mol. Biol. 215*, 635–651.
Zbiral, E., Brandstetter, H. H., & Schreiner, E. P. (1988) *Monatsh. Chem. 119*, 127–141.